

# Photoinduced Electron Transfer via Nonbuttressed Metal–Metal Bonds. The Photochemical Study of Binuclear Complexes with Platinum–Thallium Bonds

Mikhail Maliarik,<sup>\*,†</sup> Victor F. Plyusnin,<sup>‡</sup> Vjacheslav P. Grivin,<sup>‡</sup> Imre Tóth,<sup>§</sup> and Julius Glaser<sup>||</sup>

*IFM-Department of Chemistry, Linköping University, S-581 83 Linköping, Sweden, Institute of Chemical Kinetics and Combustion, Siberian Branch of the Russian Academy of Sciences, 630090 Novosibirsk, Russia, Department of Inorganic and Analytical Chemistry, University of Debrecen, Hungary, and Department of Chemistry, Royal Institute of Technology (KTH), Stockholm, Sweden*

Received: December 28, 2007; Revised Manuscript Received: April 14, 2008

The photochemistry of binuclear metal–metal bonded complexes  $[(\text{NC})_5\text{Pt}-\text{Tl}(\text{solv})_x]$  (solv is water or dimethylsulfoxide) has been studied in aqueous and dimethylsulfoxide solutions. Both stationary and nanosecond laser flash photolysis have been carried out on the species. The metal–metal bonded complexes have been photolyzed by irradiation into the corresponding intense MMCT absorption bands. Photoexcitation results in the cleavage of the platinum–thallium bond and the formation of a solvated thallos ion and a cyano complex of platinum(IV),  $[\text{Pt}(\text{CN})_5(\text{solv})]^-$ , in both cases. The species have been characterized by multinuclear NMR and optical spectroscopy. The products of the photoreaction indicate a complementary two-electron transfer occurring between platinum and thallium ions in the binuclear Pt–Tl species. Quantum yield values for the photodecomposition of the species have been determined. The intermediates of the photoinduced metal-to-metal electron transfer have been detected and characterized by optical spectroscopy. The kinetics of transient formation and decomposition have been studied, and mechanisms of the photoactivated redox reaction have been suggested.

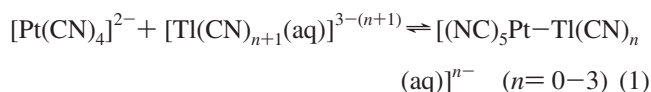
## Introduction

Photochemical investigations on nonsupported metal–metal bonds have been mostly carried out on carbonyl-containing metal–metal bonded homonuclear dimers,  $\text{M}-\text{M}$ .<sup>1–3</sup> Several instances of photosensitive heterobinuclear organometallic compounds with dative covalent bonds,  $\text{M}-\text{M}'$ , have been also reported.<sup>4–8</sup> Irradiation of the homonuclear dimers generally leads to either metal–metal bond homolysis or metal–ligand bond dissociation.<sup>2</sup> Molecules with metal–metal dative bonds are of special interest since photolysis may result in heterolytic cleavage of the  $\text{M}-\text{M}'$  bonds. The number of experimentally proven examples of the photoinduced heterolysis is, however, very limited. To the best of our knowledge, the heterolytic scission of the dative metal–metal bond has been confirmed only for  $\text{Co}-\text{Au}$  and  $\text{Os}-\text{W}$  linkages in  $[\text{Ph}_3\text{PAu}-\text{Co}(\text{CO})_4]_2^5$  and  $[(\text{Me}_3\text{P})(\text{OC})_4\text{Os}-\text{W}(\text{CO})_5]_2^8$  complexes, respectively.

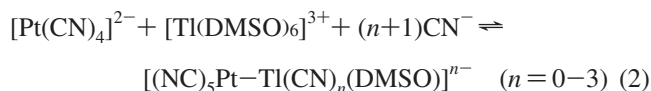
An interesting group of heteronuclear complexes, where metal–metal bonds are formed between metal ions in their reducing and oxidizing forms, has been also reported but received relatively little study.<sup>9</sup> Such a direct but polar metal–metal bond provides a very strong coupling between metals, and characteristic intense bands attributed to metal-to-metal charge transfer (MMCT) transitions are observed in the optical spectra of the compounds. Excitation of these inner-sphere MMCT transitions induces photoredox reactions between the coupled metal ions. A number of photoinduced electron transfer reactions of this type were reported by Vogler.<sup>5,10,11</sup> Furthermore, this class of coordination compounds also involves the only hitherto reported photochemically active metal–metal

bonded species not containing carbonyl ligands, namely, a trinuclear cyanide complex,  $[(\text{NC})_5\text{Co}-\text{Hg}-\text{Co}(\text{CN})_5]^{6-}$ .<sup>11</sup>

Recently we have reported studies of the formation, structure, and equilibria in a new family of oligometallic platinum–thallium cyano compounds with a direct and nonbuttressed metal–metal bond.<sup>12–15</sup> Depending on the concentration of metal ions, cyanide ion, and the pH, four binuclear species represented by the general formula  $[(\text{NC})_5\text{Pt}-\text{Tl}(\text{CN})_n(\text{aq})]^{n-}$  ( $n = 0–3$ ) and a trinuclear complex  $[(\text{NC})_5\text{Pt}-\text{Tl}-\text{Pt}(\text{CN})_5]^{3-}$  can be formed in aqueous solution. The compounds are formed via a reaction between cyano complexes of platinum(II) and thallium(III):



We have also found that similar binuclear platinum–thallium bonded compounds can be formed in dimethylsulfoxide (DMSO) solution:<sup>16,17</sup>



Both the structure of the bimetallic complexes (pseudooc-tahedral geometry of the platinum coordination) and the oxidation states of the metals, assessed by several methods, e.g., X-ray photoelectron spectroscopy (XPS) and NMR, indicate partial oxidation of platinum by thallium in the metal–metal bonded compounds.<sup>15</sup>

The compounds are usually very inert toward redox decomposition and can be kept in solution in the dark and at room temperature (295 K) for months. However, when heated or exposed to the daylight, a redox reaction between the directly linked metal ions takes place. This results in cleavage of the metal–metal bond and decomposition of the complexes. Both

\* Corresponding author.

† Linköping University.

‡ Siberian Branch of the Russian Academy of Sciences.

§ University of Debrecen.

|| Royal Institute of Technology.

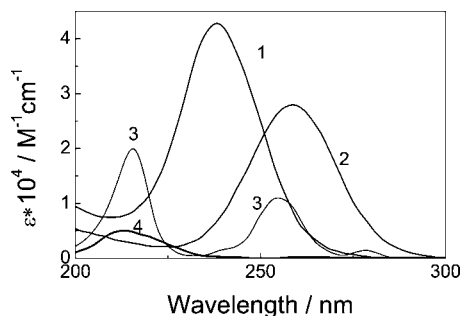
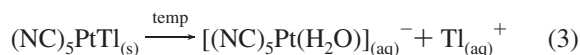
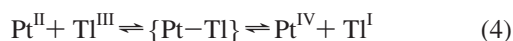


**Figure 1.** Absorption spectra of the  $[(\text{NC})_5\text{Pt}-\text{Tl}(\text{CN})_n(\text{aq})]^{n-}$  complexes and related species in aqueous solution. 1:  $[(\text{NC})_5\text{Pt}-\text{Tl}(\text{CN})_n(\text{aq})]^{n-}$ ; 2:  $[(\text{NC})_5\text{Pt}-\text{Tl}(\text{H}_2\text{O})_x]^{n-}$  (in 0.1 M  $\text{HClO}_4$ ); 3:  $[\text{Pt}(\text{CN})_4]^{2-}$  ( $\text{K}_2\text{Pt}(\text{CN})_4$ ); 4:  $\text{Tl}^+(\text{aq})$  ( $\text{Tl}^+\text{ClO}_4$  in 0.1 M  $\text{HClO}_4$ ).

thermal- and photodecomposition of the binuclear Pt–Tl species in aqueous solution give rise to monovalent thallium as the only product of thallium reduction, whereas various complexes of platinum(IV)— $[\text{Pt}(\text{CN})_6]^{2-}$ ,  $[\text{Pt}(\text{CN})_5(\text{OH})]^{2-}$ ,  $[\text{Pt}(\text{CN})_5\text{H}_2\text{O}]^-$  are formed depending on the starting Pt–Tl complex and pH. This can be illustrated by the thermal decomposition of the solid compound  $(\text{NC})_5\text{PtTl}^{18}$  in acidic aqueous solution:<sup>19</sup>



The oligometallic compounds can therefore be viewed as metastable intermediates in the course of a complementary two-electron transfer reaction between platinum(II) and thallium(III) cyano complexes stabilized by the metal–metal bond:



Our interest in photoinduced electron-transfer reactions occurring via direct metal–metal linkages led us to the detailed study of the photochemical reactions of the oligometallic platinum–thallium cyano complexes. In this paper we present the first quantitative photochemical characterization of the species belonging to this formally  $\text{Pt}^{\text{II}}-\text{Tl}^{\text{III}}$  system. Two representatives of the family of the compounds, namely, the binuclear complexes  $[(\text{NC})_5\text{Pt}-\text{Tl}(\text{H}_2\text{O})_x]$  and  $[(\text{NC})_5\text{Pt}-\text{Tl}(\text{DMSO})_x]$  in aqueous and DMSO solutions, respectively, have been studied. Both stationary and laser flash photolysis of the compounds have been carried out.

## Experimental Section

**Materials. 1.  $[(\text{NC})_5\text{Pt}-\text{Tl}(\text{H}_2\text{O})_x]$  in  $\text{H}_2\text{O}$ .** Solutions of  $[(\text{NC})_5\text{Pt}-\text{Tl}(\text{H}_2\text{O})_x]$  in 0.1 M aqueous  $\text{HClO}_4$  were prepared from powder samples of  $(\text{NC})_5\text{PtTl}$ . The synthesis and structure of the polycrystalline compound  $(\text{NC})_5\text{PtTl}$  were described in our previous publications.<sup>18,19</sup> The concentration ranges used were  $3.1 \times 10^{-4}$  to  $4.3 \times 10^{-3}$  M for optical spectroscopy and  $>10$  mM for NMR studies.

The same species,  $[(\text{NC})_5\text{Pt}-\text{Tl}(\text{H}_2\text{O})_x]$ , can be prepared in acidic aqueous solution via a reaction between the tetracyano-platinum(II) complex and thallium(III) cyanide species at  $\text{pH} \geq 4$ , followed by an increase in the acidity of the solution, down to  $\text{pH} \leq 0$ , in order to shift the equilibrium between the  $[(\text{NC})_5\text{Pt}-\text{Tl}(\text{CN})_n(\text{aq})]^{n-}$  ( $n = 0-3$ ) complexes to the species with  $n = 0$ .<sup>14</sup> The complex  $[(\text{NC})_5\text{Pt}-\text{Tl}(\text{H}_2\text{O})_x]$  cannot be obtained by the direct reaction between the platinum and thallium cyanides because of kinetic reasons.<sup>20</sup>

**2.  $[(\text{NC})_5\text{Pt}-\text{Tl}(\text{DMSO})_x]$  in DMSO.** Solutions of  $[(\text{NC})_5\text{Pt}-\text{Tl}(\text{DMSO})_x]$  in DMSO were prepared from the crystalline  $[(\text{NC})_5\text{Pt}-\text{Tl}(\text{DMSO})_4] \cdot (\text{DMSO})$  compound. Synthesis and structural characterization of the complex in solid state and in solution have been described recently.<sup>17</sup> The concentration range used was  $1.1 \times 10^{-4}$  to  $2.5 \times 10^{-3}$  M for optical spectroscopy and  $>10$  mM for NMR studies.

**Solvents.** Bidistilled water was used for preparation of all aqueous solutions. DMSO was distilled before used.

**Methods. Photolysis.** Both stationary and flash photolysis studies of the binuclear complexes were carried out with a XeCl excimer laser operating at 308 nm. The duration of the laser pulse was 10 ns with 10 mJ/pulse.

**Stationary Photolysis.** The samples of the solutions in 1 mm quartz cuvettes were irradiated by a series of laser pulses when following the disappearance of the UV–vis MMCT absorption bands at 259 and 297 nm for the complexes  $[(\text{NC})_5\text{Pt}-\text{Tl}(\text{H}_2\text{O})_x]$  and  $[(\text{NC})_5\text{Pt}-\text{Tl}(\text{DMSO})_x]$ , respectively. Absorbed light intensity at the wavelength of the laser was 6.7 and 97% for the aqueous and DMSO species, respectively. The light intensity of the laser pulse was determined by actinometry using the T–T absorption of anthracene in benzene at 431 nm ( $\epsilon = 42000 \text{ M}^{-1} \text{ cm}^{-1}$ ,  $\epsilon = 0.53^{21}$ ). Quantum yield determinations were carried out at ambient temperature.

**Laser Flash Photolysis.** Transient absorptions following 308-nm laser pulses were monitored with a 120 W pulsed xenon arc lamp (probing light). The duration of the probing pulse was 1 ms. Exciting and probing light beams were passed to the cell through a hole (2 mm in diameter) in a diaphragm. The probing light was passed through a monochromator to a pulse-supplied photomultiplier. A signal was passed to a broadband amplifier (100 MHz; gain 1–256) with compensation of the probing pulse illumination. The amplified signal was sent to an eight-bit analogue–digital recorder with a memory for 1024 readings. The minimum access time was 50 ns per reading. The details of the setup system have been described previously.<sup>22</sup> When the effect of the light intensity was studied, the laser intensity was attenuated by 1.6–63% using gray filters.

The flash photolysis studies were carried out on the samples in 10 mm quartz cuvettes kept at ambient temperature. All the solutions were deoxygenated by purging nitrogen for at least 15 min prior to the data collection. Kinetic data from at least 20 laser flashes were averaged.

In order to determine molar absorption coefficients of transient absorption bands, both flash and stationary photolysis were carried out on the same sample in a microcuvette with the size of  $2 \times 5 \times 5$  mm. In this case, the whole volume of the cuvette was exposed to the laser pulse. The decrease in the optical density of the MMCT band of the  $[(\text{NC})_5\text{Pt}-\text{Tl}(\text{solv})]$  complex in the “stationary” absorption spectra after one laser pulse ( $\Delta D_{\text{main}}$ ) and the corresponding decrease in the absorption of the transient species ( $\Delta D_{\text{trans}}$ ) in the pulse experiment were measured. The molar absorption coefficient of the transient band was calculated from the ratio  $\Delta D_{\text{trans}}/\Delta D_{\text{main}}$  and the molar absorption coefficient of the corresponding MMCT band (Table 1).

**Stationary Spectroscopy. UV–vis Spectroscopy.** UV–vis spectra of the solutions were measured with a Varian Cary-5 and HP 8453 spectrophotometers.

**NMR Spectroscopy.** All NMR measurements were performed on a Bruker DMX500 spectrometer at a probe temperature of  $298(\pm 0.5)$  K. Information on typical  $^{205}\text{Tl}$  and  $^{195}\text{Pt}$  NMR parameters for similar systems has been given in recent publications from this laboratory.<sup>13,14</sup>

**TABLE 1: Optical Properties of the Bimetallic [(NC)<sub>5</sub>Pt–Tl(solv)<sub>x</sub>] Complexes and Related Species, As Well As Optical and Kinetic Characteristics of Transients of Photodecomposition of the Pt–Tl Complexes in Solution**

complex	$\lambda_{\max}/\text{nm}$	$\epsilon/l \cdot \text{mol}^{-1}\text{cm}^{-1}$	$k_{\text{obs}}/\text{s}^{-1}$ (decay)
Bimetallic Complexes and Transient Species in H <sub>2</sub> O			
[(NC) <sub>5</sub> Pt–Tl(H <sub>2</sub> O) <sub>x</sub> ]	259	$2.9 \times 10^4$	
fast intermediate	345	$750 \pm 80$	1st-order reaction $(7.0 \pm 1.0) \times 10^4$
slow intermediate	<320	$\sim 270 \pm 50$	unestablished order $150 \pm 70$
Bimetallic Complexes and Transient Species in DMSO			
[(NC) <sub>5</sub> Pt–Tl(DMSO) <sub>x</sub> ]	297	$2.1 \times 10^4$	
fast intermediate	420	$1200 \pm 200$	1st-order reaction $(2.7 \pm 0.5) \times 10^5$
slow intermediate	410 (330 (sh))	$740 \pm 150$	2nd-order reaction $(8.2 \pm 0.3) \times 10^7 \text{ M}^{-1}\text{s}^{-1}$
Reactant (Pt <sup>2+</sup> ) and Product (Tl <sup>+</sup> ) Species in H <sub>2</sub> O and DMSO			
[Pt(CN) <sub>4</sub> ] <sub>(aq)</sub> <sup>2-</sup>	216	$2.43 \times 10^4$	
	255	$1.24 \times 10^4$	
	280	$1.77 \times 10^3$	
[Pt(CN) <sub>4</sub> ] <sub>(DMSO)</sub> <sup>2-</sup>	262	$1.95 \times 10^4$	
Tl <sup>+</sup> <sub>(aq)</sub>	213	4860	
Tl <sup>+</sup> <sub>(DMSO)</sub>	249	2600	

**TABLE 2: NMR Characterization of the Products of Photodecomposition of the Bimetallic Pt–Tl Complexes and Related Platinum and Thallium Species in Solution**

complex	solvent	<sup>195</sup> Pt (ppm)	<sup>205</sup> Tl (ppm)	<sup>1</sup> J <sub>Tl–Pt</sub> (Hz)	reference
[(NC) <sub>5</sub> Pt–Tl(solv) <sub>x</sub> ]	0.1 M HClO <sub>4</sub>	470	790	71000	13
	DMSO	570	890	66000	16, 17a
[Pt(CN) <sub>5</sub> (solv)] <sup>-</sup>	0.1 M HClO <sub>4</sub>	1767			19
	DMSO	1969			this work
[Pt(CN) <sub>4</sub> ] <sup>2-</sup>	0.1 M HClO <sub>4</sub>	-213			19
	DMSO	-190			17b
Tl <sup>+</sup> (solv)	0.1 M HClO <sub>4</sub>		5		13
	DMSO		350		16, 17a

## Results

**1. Electronic Absorption Spectra of the Pt–Tl Bonded Complexes.** A new and very intense band appears in the UV region of the electronic absorption spectra upon mixing of equimolar amounts of aqueous solutions of tetracyanoplatinum(II) and thallium(III) cyanide complexes (reaction 1). The new feature is attributed to the formation of the binuclear species [(NC)<sub>5</sub>Pt–Tl(CN)<sub>n</sub>(aq)]<sup>n-</sup> ( $n = 0-3$ ) (Figure 1). While the mononuclear [Tl(CN)<sub>n+1</sub>(aq)]<sup>3-(n+1)-</sup> species have negligible absorption in this region, the [Pt(CN)<sub>4</sub>]<sup>2-</sup> complex exhibits a number of features between 216 and 280 nm.<sup>23,24</sup> The bands of the bimetallic compounds can, however, be easily distinguished in the spectra. The stability constants for the bimetallic complexes (reaction 1) are very large ( $\log \beta = 20-45$ ),<sup>14</sup> and the equilibrium is almost completely shifted to the formation of the Pt–Tl species. Apart from this, the molar absorption coefficients of the bands of the bimetallic complexes are substantially higher compared to the bands of tetracyanoplatinate(II) ion ( $\epsilon = 2.9 \times 10^4 \text{ M}^{-1} \text{ cm}^{-1}$  at 259 nm and  $\epsilon = 4.5 \times 10^4$  at 238 nm for  $n = 0$  and 1, respectively) (Figure 1 and Table 1).

Similarly to the aqueous solutions, a new strong feature is found in the UV–vis spectra of the solutions of the bimetallic platinum complexes [(NC)<sub>5</sub>Pt–Tl(CN)<sub>n</sub>(DMSO)]<sup>n-</sup> ( $n = 0-3$ ) in DMSO. Thus the [(NC)<sub>5</sub>Pt–Tl(DMSO)<sub>x</sub>]<sub>1</sub> species ( $n = 0$ ) exhibits the absorption maximum at 297 nm with  $\epsilon = 2.1 \times 10^4 \text{ M}^{-1} \text{ cm}^{-1}$ .<sup>17a</sup>

The formation of the bimetallic compounds can be also conveniently demonstrated by NMR spectroscopy. Both <sup>195</sup>Pt and <sup>205</sup>Tl spectra of the binuclear Pt–Tl bonded complexes exhibit a very strong one-bond spin–spin coupling constant between these two nuclei (Table 2, see ref 13 for the details). Thus the <sup>1</sup>J<sub>Tl–Pt</sub> for the studied [(NC)<sub>5</sub>Pt–Tl(solv)<sub>x</sub>]<sub>1</sub> complexes is 71 and 66 kHz for the aqueous and DMSO species, respectively.

**2. Stationary Photolysis of the [(NC)<sub>5</sub>Pt–Tl(solv)] Complexes.** Steady-state photolysis of the [(NC)<sub>5</sub>Pt–Tl(H<sub>2</sub>O)<sub>x</sub>]<sub>1</sub> complex in acidic aqueous solution results in a continuous decrease in the intensity of the band at 259 nm in the electronic absorption spectra (Figure 2). Degradation of this band is accompanied by the appearance of a new absorption at  $\sim 213$  nm. The quantum yield of the photodecomposition of the complex was calculated to be  $(9.1 \pm 0.1) \times 10^{-3}$ .

Similarly to the aqueated Pt–Tl complex, stationary photolysis of the [(NC)<sub>5</sub>Pt–Tl(DMSO)<sub>x</sub>]<sub>1</sub> species in the DMSO solution causes a continuous decline in the characteristic band at 297 nm (Figure 3). No new bands appearing in the course of photoreaction could be detected in the range of wavelengths “transparent” for DMSO ( $>250$  nm). At the same time, the absorption clearly grows at the shorter wavelengths ( $\leq 250$  nm)

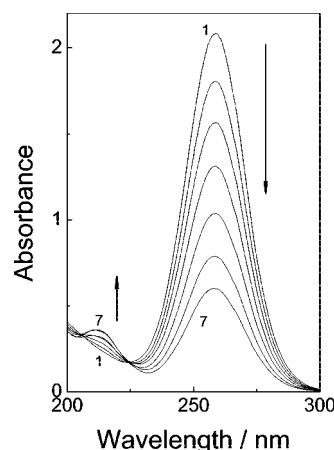


**Figure 2.** Absorption spectra of the [(NC)<sub>5</sub>Pt–Tl(H<sub>2</sub>O)<sub>x</sub>]<sub>1</sub> complex ( $7.2 \times 10^{-4} \text{ M}$  in 0.1 M HClO<sub>4</sub>,  $l = 0.1 \text{ cm}$ ) following stationary photolysis. The solution was flashed with a 308-nm laser. Spectra 1–7: 0, 10, 20, 40, 80, 150, and 300 laser pulses, respectively.

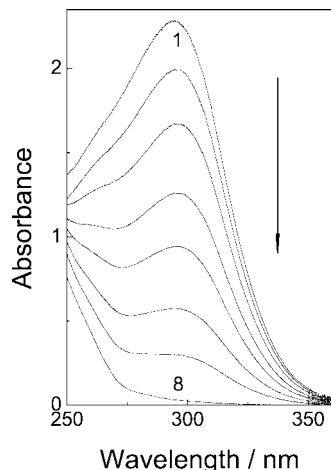


**Figure 3.** Absorption spectra of the  $[(\text{NC})_5\text{Pt-Tl}(\text{DMSO})_x]$  complex ( $1.1 \times 10^{-3}$  M,  $l = 0.1$  cm) in DMSO solution following stationary photolysis. The solution was flashed with a 308-nm laser. Spectra 1–8: 0, 2, 5, 10, 15, 20, 40, and 100 laser pulses, respectively.

(Figure 3). The maximum of the resulting absorption of the photolyzed solution can be fitted to  $\sim 250$  nm. The overall quantum yield of the photodegradation was calculated to be  $(4.6 \pm 0.1) \times 10^{-3}$ .

Photolysis of the solutions of the  $[(\text{NC})_5\text{Pt-Tl}(\text{sol})]$  complexes in the concentration range of  $>10$  mM is conveniently followed by  $^{205}\text{Tl}$  NMR spectra. The intensity of the  $^{205}\text{Tl}$  NMR signal of the bimetallic complex decreases continuously, accompanied by growing of the signal of the solvated thallos ion (Table 2). Transformation of thallium from one species to another is quantitative; no other thallium products of the photodecomposition are found in the  $^{205}\text{Tl}$  spectra.  $^{195}\text{Pt}$  NMR spectra of the photolyzed solutions of the  $[(\text{NC})_5\text{Pt-Tl}(\text{sol})]$  complexes (0.02–0.05 M) exhibit only signals of the  $[(\text{NC})_5\text{Pt}(\text{H}_2\text{O})]^-$  and  $[(\text{NC})_5\text{Pt}(\text{DMSO})]^-$  species in acidic aqueous and DMSO solutions, respectively (Table 2).

**3. Time-Resolved Spectroscopy of the  $[(\text{NC})_5\text{Pt-Tl}(\text{sol})]$  Complexes in Solution. 3.1. Laser Flash Photolysis of the  $[(\text{NC})_5\text{Pt-Tl}(\text{aq})]$  Complex in Acidic Aqueous Solution.** A new broadband with a maximum at 345 nm appears in the transient absorption spectrum of the aqueous solution of the  $[(\text{NC})_5\text{Pt-Tl}(\text{aq})]$  complex induced by a 308-nm laser pulse (Figure 4). The molar absorption coefficient of the band has been calculated:  $\epsilon_{345} = 750 \pm 80 \text{ M}^{-1}\text{cm}^{-1}$  (see the Experimental Section for the details). The transient absorption is continuously blue-shifted with time. Thus after 50  $\mu\text{s}$ , the 345 nm band is transformed to a new less intensive absorption with the maximum located at  $\lambda \sim 320$  nm (Figure 4). The kinetic traces of the transient absorption at 345 nm show that the latter feature decays on a tens of milliseconds time scale (Figure 5).

The 345 nm kinetic trace on a 100  $\mu\text{s}$  time scale can be fit reasonably well with a single exponential decay (the bold solid line in Figure 5a), giving an observed rate constant  $k_{\text{fast}} = (7.0 \pm 1.0) \times 10^4 \text{ s}^{-1}$ . Plotting the pseudo-first-order rate constant against the amplitude of the transient absorption signal at 345 nm for the “fast” component of the kinetics shows the independence of the  $k_{\text{fast}}$  value on  $\Delta D_{345}$ . This testifies that the transient absorption decays in accordance with the first-order kinetics.

The nascent secondary transient absorption band with  $\lambda_{\text{max}} \sim 320$  nm decays with a rate constant of two to three orders of magnitude lower,  $k_{\text{slow}} = 150 \pm 70 \text{ s}^{-1}$ . The rate constant of this “slow” process has been obtained by fitting the kinetic trace

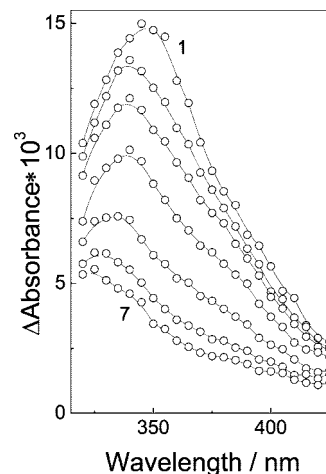


**Figure 4.** Transient absorption spectra following 308-nm laser flash photolysis of the  $[(\text{NC})_5\text{Pt-Tl}(\text{H}_2\text{O})_x]$  complex ( $3.1 \times 10^{-4}$  M in 0.1 M  $\text{HClO}_4$ ). Spectra 1–7: 0, 3.2, 6.4, 12.8, 25.6, 51.2, and 190  $\mu\text{s}$  after the laser pulse.

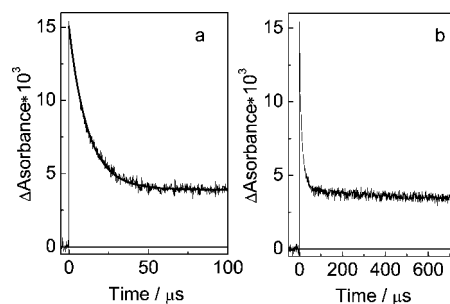


**Figure 5.** Kinetic profiles of the transient absorption at 345 nm of the  $[(\text{NC})_5\text{Pt-Tl}(\text{H}_2\text{O})_x]$  complex ( $3.1 \times 10^{-4}$  M in 0.1 M  $\text{HClO}_4$ ) flashed by a 308-nm laser. Transient traces at (a) 100 and (b) 800  $\mu\text{s}$  time scales are shown. The bold solid line indicates the best fit to a single exponential decay.

in the 200–800  $\mu\text{s}$  time range to a single exponential decay (Figure 5b). Small amplitudes of the transient absorption of the slow component prevent performing accurate measurements to establish the order of the rate law.

**3.2. Laser Flash Photolysis of the  $[(\text{NC})_5\text{Pt-Tl}(\text{DMSO})_x]$  Complex in DMSO Solution.** As in the case of the  $[(\text{NC})_5\text{Pt-Tl}(\text{aq})]$  complex in water, a transient absorption was detected in the flash photolysis of the  $[(\text{NC})_5\text{Pt-Tl}(\text{DMSO})_x]$  species in DMSO solution. A band centered at  $\sim 420$  nm appears in the transient spectra following the laser pulse (Figure 6). The molar absorption coefficient,  $\epsilon_{420} = 1200 \pm 200 \text{ M}^{-1}\text{cm}^{-1}$ , was calculated for the band. Similar to the stationary optical spectra, the bands in the transient absorption spectra of the DMSO complex are shifted to red compared to the aqueous complex.

Furthermore, as in the case of the aqueous complex, the transient absorption of the DMSO species is vanished in two stages. The first stage is fast and is completed within  $\sim 20$   $\mu\text{s}$ . By this time, the intensity of the 420 nm band is decreased by  $\sim 30\%$ . The decay of the 420 nm absorption is accompanied, however, by the increase of the optical density at the wavelength  $\lambda < 345$  nm, which gives rise to a shoulder at  $\sim 330$  nm. An isosbestic point at 345 nm is also detected, which implies mutual relation between these two bands (Figure 6). The maximum of the transient absorption is shifted by this moment to about 410 nm. In the range of wavelengths around 300 nm, where the complex  $[(\text{NC})_5\text{Pt-Tl}(\text{DMSO})_x]$  has a strong absorption band (Figure 3), the disappearance of transient species is accompanied by the decrease of the optical density.

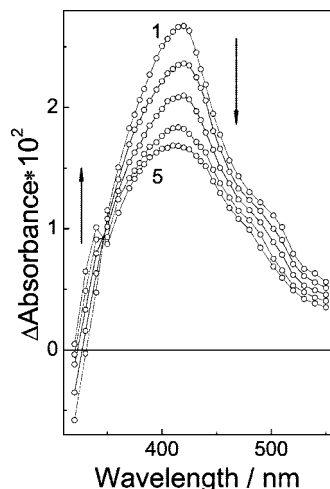


**Figure 6.** Transient absorption spectra following 308 nm laser flash photolysis of the  $[(\text{NC})_5\text{Pt-Tl}(\text{DMSO})_x]$  complex ( $1.2 \times 10^{-4}$  M) in DMSO solution. Spectra 1–5: 0, 1.6, 6.4, 25.6, and 48.0  $\mu\text{s}$ , respectively, after the laser pulse.

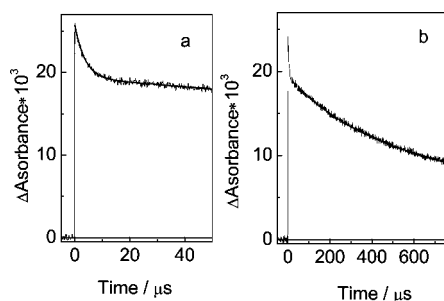


**Figure 7.** Kinetic profiles of the transient absorption at 420 nm of the  $[(\text{NC})_5\text{Pt-Tl}(\text{DMSO})_x]$  complex ( $1.2 \times 10^{-4}$  M) in DMSO solution flashed by a 308-nm laser. Transient traces at (a) 50 and (b) 800  $\mu\text{s}$  time scales are shown. The bold solid line indicates the best fit to single exponential (a) and second-order (b) decay functions.

The kinetic traces of the transient absorption at 420 nm obtained at two time scales, 50 and 800  $\mu\text{s}$ , are shown in Figure 7. None of the traces can be well fit to simple first- or second-order decay functions. The decay profiles at the shorter time scale can, however, be successfully treated with a two exponential model:

$$\Delta D(t) = A_1 e^{-k_{\text{fast}} t} + A_2 e^{-k_{\text{slow}} t}$$

giving a very reasonable fit (the bold solid line in Figure 7a). The fitting shows that the rate constant of the fast process,  $k_{\text{fast}} = (2.7 \pm 0.5) \times 10^5 \text{ s}^{-1}$ , does not depend on the initial optical density after the laser pulse ( $A_1 + A_2$ ). This independence indicates that decay of the intermediate complex occurs in accordance with first-order kinetics. The observed rate constant for the slow process,  $k_{\text{slow}} = (1.4 \pm 0.2) \times 10^3 \text{ s}^{-1}$ , on the other hand, does show dependence on the initial signal amplitude ( $A_2$ ), *vide infra*. It can be noted that, in the case of DMSO solutions, both fast and slow processes occur faster compared to those in water solutions (Table 1).

In order to obtain more accurate data on the kinetics of the slow process and to establish the order of the reaction, the decay profiles at the longer time scale, 800  $\mu\text{s}$ , were also analyzed (Figure 7b). It was found that the kinetic traces in the 20–800  $\mu\text{s}$  time domain obey the second-order rate law (bold solid line in Figure 7b). Moreover, Figure 8 shows that  $k_{\text{slow}}$  depends linearly on the amplitude of the signal. The linear fit passing through the origin indicates a purely second-order reaction. The

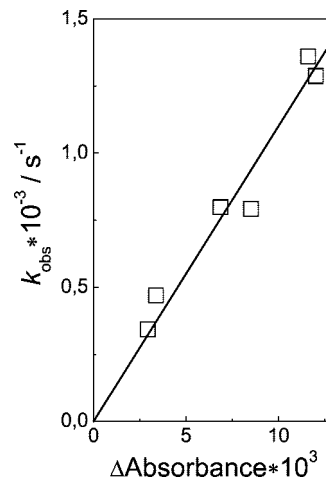


**Figure 8.** The plot of the observed rate constant,  $k_{\text{obs}}$  ( $k_{\text{slow}}$ ), of the transient absorption decay profiles at 420 nm following 308-nm laser irradiation of the  $[(\text{NC})_5\text{Pt-Tl}(\text{DMSO})_x]$  complex ( $1.2 \times 10^{-4}$  M) in DMSO solution vs the initial transient absorbance.

bimolecular rate constant ( $k_{\text{bim}}$ ) was calculated from the slope of the linear plot (see Table 1).

## Discussion

**The MMCT Absorption Bands.** The very large molar absorption coefficients of the bands (exceeding  $10^4$  in all cases) in the electron absorption spectra of the Pt–Tl complexes point to a substantial change in the instantaneous dipole moment accompanying the electronic transition, which usually serves as an indication of charge transfer excitations.<sup>25,26</sup> The charge-transfer character of the transition is further confirmed by observation of solvatochromic behavior of the absorption band.<sup>27,28</sup> In the present case, it is less probable that the formation of a metal–metal bond would strongly enhance ligand-to-metal (LMCT) or metal-to-ligand (MLCT) charge transfer transitions. We therefore believe that the intense optical bands in the spectra of binuclear complexes arise from the MMCT excitation.<sup>9</sup>

To the best of our knowledge, the only example of the MMCT transition in heterobinuclear complexes with an unsupported polar metal–metal bond reported so far was complex  $[\text{Ph}_3\text{PAu}^{\text{I}}-\text{Co}^{\text{I}}(\text{CO})_4]$ , which exhibited a  $\text{Co}(\text{I}) \rightarrow \text{Au}(\text{I})$  MMCT band in the absorption spectra.<sup>5</sup>

**Photochemical Characterization of the Binuclear Complexes  $[(\text{NC})_5\text{Pt-Tl}(\text{sol})]$  in Solution.** According to the thermally induced decomposition of the  $[(\text{NC})_5\text{Pt-Tl}(\text{aq})]$  compound in the acidic aqueous solution (reaction 3), a pentacyano complex of platinum(IV) and monovalent thallium are formed as the final products of the redox reaction between the two coupled metal ions. The products were detected by  $^{195}\text{Pt}$  and  $^{205}\text{Tl}$  NMR.<sup>19</sup> The same platinum and thallium species are also found in the photolyzed sample of the binuclear complex in the concentration range 20–50 mM (Table 2).

Disappearance of the strong MMCT band in the electronic absorption spectra of the diluted ( $\sim 10^{-4}$ – $10^{-3}$  M) solutions of the bimetallic complexes during the photolysis can itself serve as an indication of the cleavage of the Pt–Tl bond. While the  $[(\text{NC})_5\text{Pt}(\text{H}_2\text{O})]^-$  species does not display a well-defined maximum in the studied wavelength range, the  $\text{Tl}_{\text{aq}}^+$  exhibits an intense broadband centered in the far UV range,

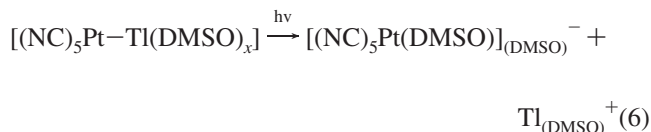
$\lambda = 213$  nm with  $\varepsilon_{213} = 4860 \text{ M}^{-1}\text{cm}^{-1}$  (Figure 1 and Table 1).<sup>29</sup> Therefore, the band with growing intensity, appearing in the optical spectra of the photolyzed  $[(\text{NC})_5\text{Pt-Tl}(\text{aq})]$  species at 213 nm, should be attributed to the aquated thallous ion (Figure 2).

The products of the decomposition of the bimetallic complex at higher concentrations (20–50 mM), obtained by both the thermal and photoinduced reactions (Table 2), point unambiguously to the complete electron transfer reaction between the coupled platinum and thallium ions accompanying the scission of the metal–metal bond. One can suppose that the same  $[(\text{NC})_5\text{Pt}(\text{H}_2\text{O})]^-$  complex is also formed as a result of photodecomposition of the bimetallic species, as a counterpart to the  $\text{Tl}_{\text{aq}}^+$  ion, at lower concentration of the complex ( $\leq 10^{-3}$  M) and at pH = 1. The overall photoinduced redox reaction for the complex  $[(\text{NC})_5\text{Pt-Tl}(\text{aq})]$  therefore resembles the thermal process (reaction 3):



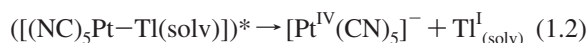
As in the case of the photoredox process in aqueous solution, the thallous ion is formed as the final product of thallium reduction in the course of the photolysis of the  $[(\text{NC})_5\text{Pt-Tl}(\text{DMSO})_x]$  complex in DMSO. The thallous ion is readily detected in the <sup>205</sup>Tl NMR spectra of the 40 mM solution (Table 2). Furthermore, similarly to the situation in water, oxidation of platinum in the presence of DMSO can be expected to give a monosolvated complex of Pt<sup>IV</sup>,  $[(\text{NC})_5\text{Pt}(\text{DMSO})]^-$ . The species has been observed in the <sup>195</sup>Pt NMR spectra of the solution (Table 2).

The results of the photolysis of the diluted ( $\leq 1$  mM) DMSO solution of the  $[(\text{NC})_5\text{Pt-Tl}(\text{DMSO})_x]$  complex have been followed by optical spectroscopy. Solvated thallous ion exhibits a band at 249 nm ( $\varepsilon = 2600 \text{ M}^{-1}\text{cm}^{-1}$ ) in DMSO solution.<sup>30</sup> The growing band centered at  $\sim 250$  nm in the spectrum of the photolyzed Pt–Tl solution can be therefore attributed to the  $\text{Tl}^+$  ion formed after decomposition of the metal–metal bonded species (Figure 3). However, the absorption of the band is at least 3 times higher compared to the value expected for the given concentration of the thallous ion and its  $\varepsilon^{249}$  in the DMSO solution. One can assume that the  $[(\text{NC})_5\text{Pt}(\text{DMSO})]^-$  species has a notable absorption in this spectral range as well. The overall photoredox reaction of the  $[(\text{NC})_5\text{Pt-Tl}(\text{DMSO})_x]$  complex in DMSO solution can be therefore presented by the following process:

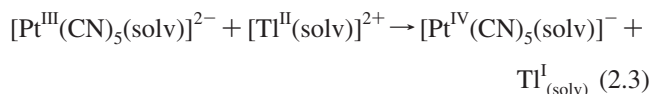
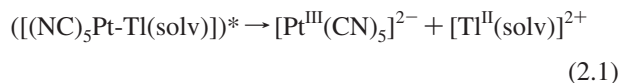


**Mechanistic Considerations.** Considering scission of the metal–metal bond is the first step of the degradation of the excited complexes  $([(\text{NC})_5\text{Pt-Tl}(\text{solvent})_x])^*$ , two mechanisms can be suggested: with heterolytic and homolytic cleavage of the Pt–Tl bond (Schemes 1 and 2, respectively).

#### Scheme 1: Heterolysis



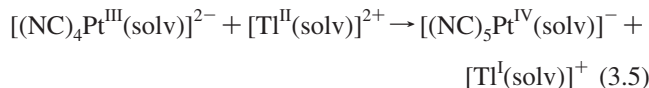
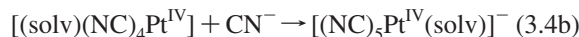
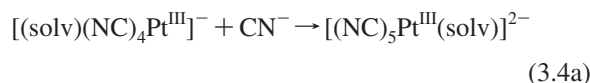
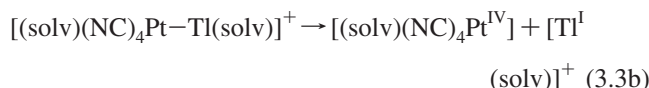
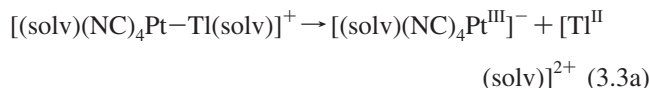
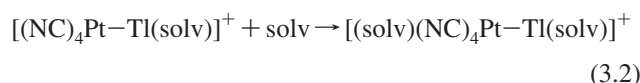
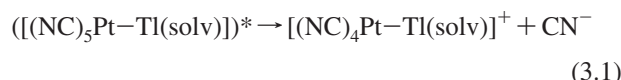
#### Scheme 2: Homolysis



According to Scheme 1, only one intermediate, a coordinatively unsaturated  $[\text{Pt}^{\text{IV}}(\text{CN})_5]^-$  species, is formed, which is not consistent with the number of the observed transient features either in aqueous or DMSO solutions. Scheme 2 can, in principle, account for the number of the observed transients; however, the kinetics of their disappearance is compatible only for the photodecomposition of the DMSO species, *vide supra*. Furthermore, disruption of the metal–metal bond at the first step of the mechanism would inevitably yield nonsolvated pentacyano species of trivalent platinum (reaction 2.1). The species is expected to give the same absorption spectra independently on the solvent used. Comparing the results of the flash photolysis of the  $[(\text{NC})_5\text{Pt-Tl}(\text{H}_2\text{O})_x]$  and  $[(\text{NC})_5\text{Pt-Tl}(\text{DMSO})_x]$  complexes, one can see that there is no common absorption feature appearing in the transient spectra of the complexes (Table 1). Formation of such intermediates as  $[\text{Pt}^{\text{III}}(\text{CN})_5]^{2-}$  (or  $[\text{Pt}^{\text{IV}}(\text{CN})_5]^-$  in Scheme 1) can therefore be excluded, at least if it is the same mechanism of photodecomposition, which operates for both bimetallic complexes.

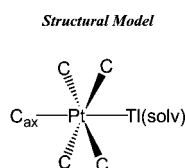
In order to account for the experimental findings and assuming the same mechanism operating for the photolysis of the  $[(\text{NC})_5\text{Pt-Tl}(\text{H}_2\text{O})_x]$  and  $[(\text{NC})_5\text{Pt-Tl}(\text{DMSO})_x]$  complexes, an alternative model can be suggested (Scheme 3).

#### Scheme 3: CN<sup>-</sup>-Ligand Removal



We suppose that cleavage of the apical Pt–CN bond can compete with disruption of the Pt–Tl bond in the excited complexes  $([(\text{NC})_5\text{Pt-Tl}(\text{solvent})])^*$ . Because of a notable bond delocalization occurring in the three-center linear  $\text{C}_{\text{ax}}-\text{Pt}-\text{Tl}$  pattern of the complex (see the Structural Model),<sup>15,31</sup> appearing in an abnormally strong coupling between the thallium and the

carbon atom in the axial position of the platinum coordination,<sup>13</sup> one can expect that the C<sub>ax</sub>–Pt bonding should be very sensitive to the MMCT excitation. The platinum–carbon bond is then supposed to be cleaved prior to the scission of the metal–metal bond. This situation is not unusual. It has been observed for a series of heteronuclear carbonyl compounds with metal–metal bonds between transition and main group IV metals that M–M' bonds are not efficiently cleaved compared to the disruption of the M–CO bonds.<sup>4</sup>



*The nitrogen atoms in the [(NC)<sub>5</sub>Pt–Tl(solv)] unit are omitted for clarity.*

Disruption of the C<sub>ax</sub>–Pt bond in the [(NC)<sub>5</sub>Pt–Tl(solv)] complexes is then followed by solvation of the coordinately unsaturated platinum center (reaction 3.2). Cleavage of the Pt–Tl bond takes place at the next step and can occur either in homo- or heterolytic fashion (reactions 3.3a and 3.3b, respectively). A vacant sixth position of the coordination of the oxidized platinum is finally filled in the reaction with the free cyanide ion (reaction 3.4). In the case of the homolytic cleavage of the Pt–Tl bond, completion of the redox reaction is also required. An electron can then be fast-transferred between the two metal complexes in an outer-sphere fashion (reaction 3.5).

In the model illustrated by Scheme 3, a sufficient number of intermediate species is formed to account for the transient features detected in the optical spectra. It is also possible to justify the observed kinetics of the intermediates formed both in aqueous and DMSO solutions. Thus, in the case of photodegradation of the [(NC)<sub>5</sub>Pt–Tl(H<sub>2</sub>O)<sub>x</sub>] complex, one can tentatively assign the 345 nm absorption to the [(NC)<sub>4</sub>Pt–Tl(aq)]<sup>+</sup> species. By means of the reaction with the solvent, the complex is transformed in the pseudo-first-order reaction to the species with the aquated platinum center, [(aq)(NC)<sub>4</sub>Pt–Tl(aq)]<sup>+</sup>, giving a broad absorption at ~320 nm (reaction 3.2). The latter is in turn decaying with the first-order kinetics accompanying the cleavage of the metal–metal bond (reaction 3.3).

Considering the photoreaction of the [(NC)<sub>5</sub>Pt–Tl(DMSO)<sub>x</sub>] complex and attempting to account for both the first- and second-order behavior of the transient features, one can assign the absorption at 420 nm rather to the [(DMSO)(NC)<sub>4</sub>Pt–Tl(DMSO)]<sup>+</sup> species. The decomposition of the bimetallic complex into homonuclear components follows the first-order kinetics. The transient platinum species then reacts with cyanide in the second-order process. Heterolytic cleavage of the Pt–Tl bond seems to be preferable for both the aqueous and DMSO complexes (reaction 3.3b), since consideration of another bimolecular reaction (3.5) can then be avoided.

## Conclusions

For the first time the quantitative photochemical characterization of several members of the family of heterometallic platinum–thallium bonded cyanide compounds has been undertaken. Both stationary and nanosecond laser flash photolysis have been applied to study photoinduced electron transfer reactions of the complexes [(NC)<sub>5</sub>Pt–Tl(H<sub>2</sub>O)<sub>x</sub>] and [(NC)<sub>5</sub>Pt–Tl(DMSO)<sub>x</sub>] in aqueous and DMSO solutions, respectively.

Irradiation of the complexes into their MMCT absorption bands results in cleavage of the metal–metal bond and irreversible redox reaction between the coupled metal ions. The products of the photodecomposition have been characterized by means of multinuclear NMR and optical spectroscopy. Values of quantum yields of the photodecomposition of the bimetallic species have been determined. The binuclear complex photolyses with  $\Phi = 9.1 \times 10^{-3}$  and  $4.6 \times 10^{-3}$  in aqueous and DMSO solutions, respectively. The intermediates of the photoinduced metal-to-metal electron transfer have been detected and characterized by optical spectroscopy. Mechanisms of the photo-activated redox reaction have been suggested. We suppose that scission of the metal–metal bond is preceded by cleavage of the axial platinum–carbon bond (Pt–CN). Disruption of the Pt–Tl bond takes place in a heterolytic fashion.

**Acknowledgment.** Financial support from the Royal Swedish Academy of Sciences is greatly acknowledged. The work has been also supported by the Russian Foundation of Basic Researches (Grants 05-03-32474, 06-03-32110, 06-03-90890-Mol, 05-03-39007GFEN, and 07-02-91016 AF), Program of Integration Projects of SB RAS (Grants 4.16 and 77), and Hungarian OTKA K63388.

## References and Notes

- (1) Meyer, T. J.; Casper, J. V. *Chem. Rev.* **1985**, *85*, 187.
- (2) Geoffroy, G. L.; Wrighton, M. S. *Organometallic Photochemistry*; Academic Press: New York, 1979.
- (3) Avey, A.; Tenhaeff, S. C.; Weakley, T. J. R.; Tyler, D. R. *Organometallics* **1991**, *10*, 3607.
- (4) Wrighton, M. S.; Graff, J. L.; Luong, J. C.; Reichel, C. L.; Robbins, J. L. *ACS Symp. Ser.* **1981**, *155*, 85.
- (5) Vogler, A.; H., K. *Z. Naturforsch.* **1989**, *44b*, 132.
- (6) Male, J. L.; Davis, H. B.; Pomeroy, R. K.; Tyler, D. R. *J. Am. Chem. Soc.* **1994**, *116*, 9353.
- (7) Male, J. L.; Einstein, F. W. B.; Leong, W. K.; Pomeroy, R. K.; Tyler, D. R. *J. Organomet. Chem.* **1997**, *549*, 105.
- (8) Male, J. L.; Pomeroy, R. K.; Tyler, D. R. *Organometallics* **1997**, *16*, 3431.
- (9) Vogler, A.; Kunkely, H. In *Photosensitization and Photocatalysis Using Inorganic and Organometallic Compounds*; Kalyanasundaram, K., Grätzel, M., Eds.; Kluwer Academic Publisher: Dordrecht, The Netherlands, 1993; Vol. 14, p 79.
- (10) Vogler, A.; H., K. *J. Organomet. Chem.* **1988**, *355*, 1.
- (11) Kunkely, H.; Stochel, G.; Vogler, A. *Z. Naturforsch.* **1989**, *44b*, 145.
- (12) Berg, K. E.; Glaser, J.; Read, M. C.; Toth, I. *J. Am. Chem. Soc.* **1995**, *117*, 7550.
- (13) Maliarik, M.; Berg, K.; Glaser, J.; Sandstrom, M.; Toth, I. *Inorg. Chem.* **1998**, *37*, 2910.
- (14) Maliarik, M.; Glaser, J.; Toth, I.; Webba da Silva, M.; Zekany, L. *Eur. J. Inorg. Chem.* **1998**, 565.
- (15) (a) Jalilehvand, F.; Maliarik, M.; Sandström, M.; Mink, J.; Persson, I.; Persson, P.; Tóth, I.; Glaser, J. *Inorg. Chem.* **2001**, *40*, 3889. (b) Chen, W.; Liu, F.; Matsumoto, K.; Autschbach, J.; Le Guennic, B.; Ziegler, T.; Maliarik, M.; Glaser, J. *Inorg. Chem.* **2006**, *45*, 4526.
- (16) Ma, G.; Kritikos, M.; Glaser, J. *Eur. J. Inorg. Chem.* **2001**, *5*, 1311.
- (17) (a) Ma, G.; Kritikos, M.; Maliarik, M.; Glaser, J. *Inorg. Chem. Acta* **2004**, *43*, 4328. (b) Ma, G.; Maliarik, M.; Sun, L.; Glaser, J. *Inorg. Chim. Acta* **2004**, *357*, 4077.
- (18) Jalilehvand, F.; Eriksson, L.; Glaser, J.; Maliarik, M.; Mink, J.; Sandström, M.; Tóth, I.; Tóth, J. *Chem.—Eur. J.* **2001**, *7*, 2167.
- (19) Maliarik, M.; Glaser, J.; Toth, I. *Inorg. Chem.* **1998**, *37*, 5452.
- (20) Nagy, P.; Toth, I.; Fabian, I.; Maliarik, M.; Glaser, J. *Inorg. Chem.* **2004**, *43*, 5216.
- (21) Compton, R. H.; Grattan, K. T. V.; Morrow, T. J. *Photochem.* **1980**, *14*, 61.
- (22) (a) Grivin, V. P.; Plyusnin, V. F.; Khmelinski, I. V.; Bazhin, N. M.; Mitewa, M.; Bontchev, P. R. *J. Photochem. Photobiol. A: Chem.* **1990**, *51*, 371. (b) Grivin, V. P.; Khmelinski, I. V.; Plyusnin, V. F.; Blinov, I. I.; Balashev, K. P. *J. Photochem. Photobiol. A: Chem.* **1990**, *51*, 167.
- (23) Giellmann, G.; Yershin, H. *Struct. Bonding (Berlin)* **1985**, *62*, 87.
- (24) Schindler, J. W.; Fukuda, R. C.; Adamson, A. W. *J. Am. Chem. Soc.* **1982**, *104*, 3596.
- (25) Horvath, O.; Stevenson, K. L. *Charge Transfer Photochemistry of Coordination Compounds*; VCH Publishers: New York, 1993.

(26) Suppan, P. *Chemistry and Light*; The Royal Society of Chemistry: Cambridge, 1994.

(27) Maliarik, M. Compounds with non-butressed metal–metal bond between platinum and thallium. Model systems for photoinduced two-electron transfer. Ph.D. Thesis, The Royal Institute of Technology, Stockholm, Sweden, 2001, p 96.

(28) Lever, A. B. P. *Inorganic Electronic Spectroscopy*; Elsevier: Amsterdam, 1984; Vol. 33.

(29) Mason, W. R. *Inorg. Chem.* **1985**, 24, 2118.

(30) Solution of  $\text{TlNO}_3$  in DMSO.

(31) Autschbach, J.; Ziegler, T. *J. Am. Chem. Soc.* **2001**, 123, 5320.

JP7121278